Supplementary Information for Reaction Landscape of a Mononuclear Mn^{III}-hydroxo Complex with Hydrogen Peroxide

Elizabeth N. Grotemeyer, Joshua D. Parham†, and Timothy A. Jackson*

The University of Kansas, Department of Chemistry and Center for Environmentally Beneficial Catalysis, 1567 Irving Hill Road, Lawrence, KS 66045, USA.

*To whom correspondence should be addressed:
Timothy A. Jackson
Phone: (785) 864-3968
taj@ku.edu

†Current address: Department of Physical Sciences, University of Central Missouri, Warrensburg, MO 64093.

Table S1. Comparison of spectroscopic characteristics of select bis(μ-oxo)dimanganese(III,IV) complexes.

Complex	***λ (nm)***	***g***	***A (mT)***	**Pre-edge Energy (eV)**	**Pre-edge area**	**Edge energy (eV)**	***Ref.***
$[Mn^{II}(dpaq^{2Me})]^{+}$	500	2.04	*NA*[b]	6540.2	4.3	6548.6	*1*
1	515, 770	*NA*[c]	*NA*[c]	6540.2	4.1	6550.0	*1*
2	500, 710	2.01	7.7	6540.9 6542.6	19.4	6550.2	*This work*
3	610, 770	*NA*[c]	*NA*[c]	6540.3	6.3	6550.5	*This work*
$[Mn^{III}Mn^{IV}(\mu\text{-}O)_2(N4Py)_2]^{3+}$	439, 562, 667	2.01	7.7	6540.3 6542.0	22.9	6549.8	*2*
$[Mn^{III}Mn^{IV}(\mu\text{-}O)_2(^{DMM}N4Py)_2]^{3+}$	440, 562, 667	2.01	7.7	6540.3 6542.0	19.6	6549.8	*3*
$[Mn^{III}Mn^{IV}(\mu\text{-}O)_2(dpaq)_2]^{+}$	540, 660	1.996	$A_x = 16.7$[a] $A_y = 14.9$[a] $A_z = 14.3$[a]	*NA*[d]	*NA*[d]	*NA*[d]	*4*

[a] From simulation of the experimental spectrum. [b]Hyperfine splitting was not resolved. [c]**1** is EPR silent. [d]XAS has not been performed on this complex.

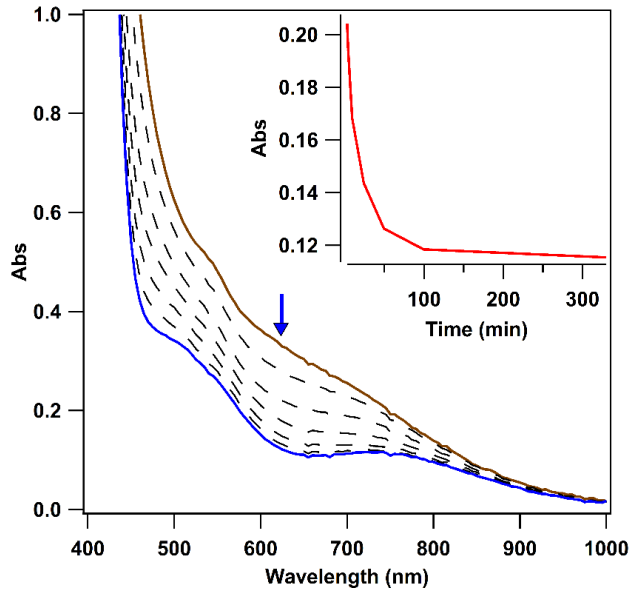

Figure S1. Electronic absorption spectra obtained while monitoring the thermal decay of $[Mn^{III}Mn^{IV}(\mu\text{-}O)_2(dpaq)_2]^{+}$ (brown trace) to yield $[Mn^{III}(OH)(dpaq)]^{+}$ (blue trace). Inset: time course of the decay.

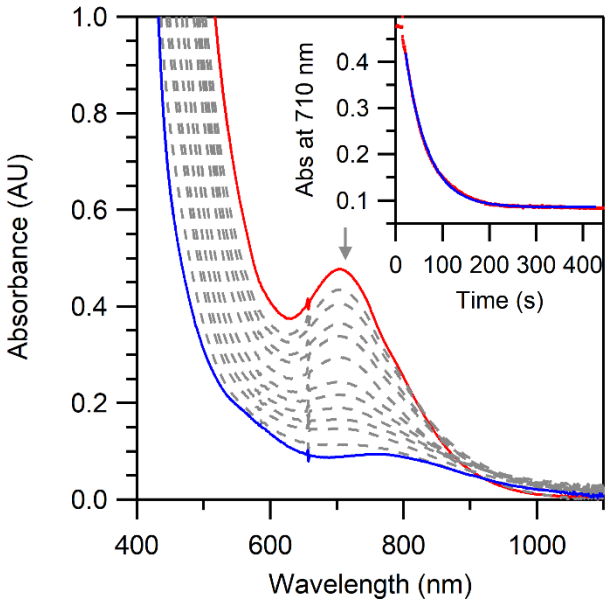

Figure S2. Top: Electronic absorption spectra for a solution of **2** (red trace) after addition of 100 equiv. 2,4-di-*tert*-butylphenol at 25°C. The feature at 710 nm decays completely to the blue trace. Inset: Decay trace of the feature at 710 nm over time.

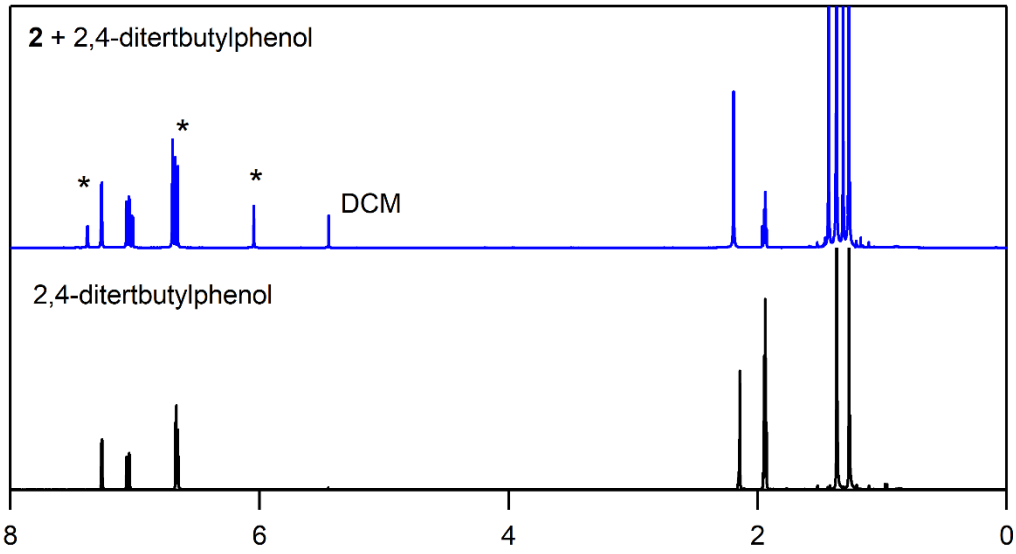

Figure S3. ^{1}H NMR spectrum for the organic products resulting from the reactions of a 1.25 mM solution of **2** with 5 equiv. 2,4-di-*tert*-butylphenol (blue trace). The ^{1}H NMR spectrum of 2,4- di-*tert*-butylphenol is included for comparison. Peaks marked with (*) arise from the dimeric reaction product 3, 3', 5, 5'-*tetra*-*tert*-butylbiphenyl-2 2'-diol.

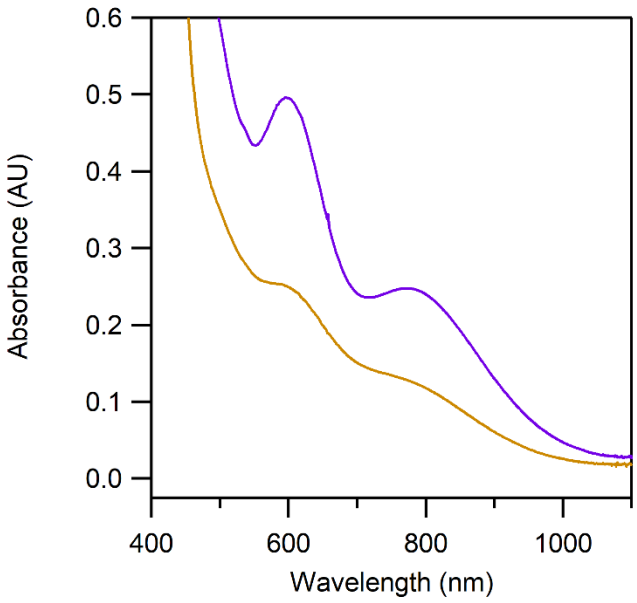

Figure S4. Overlay of the electronic absorption spectra for the intermediate in the formation of **2** by the addition of 10 equiv. H_2O_2 (brown-green trace) at 25°C and **3** formed by the addition of 5 equiv. H_2O_2 and 0.1 equiv. $HClO_4$ at -40°C (purple trace).

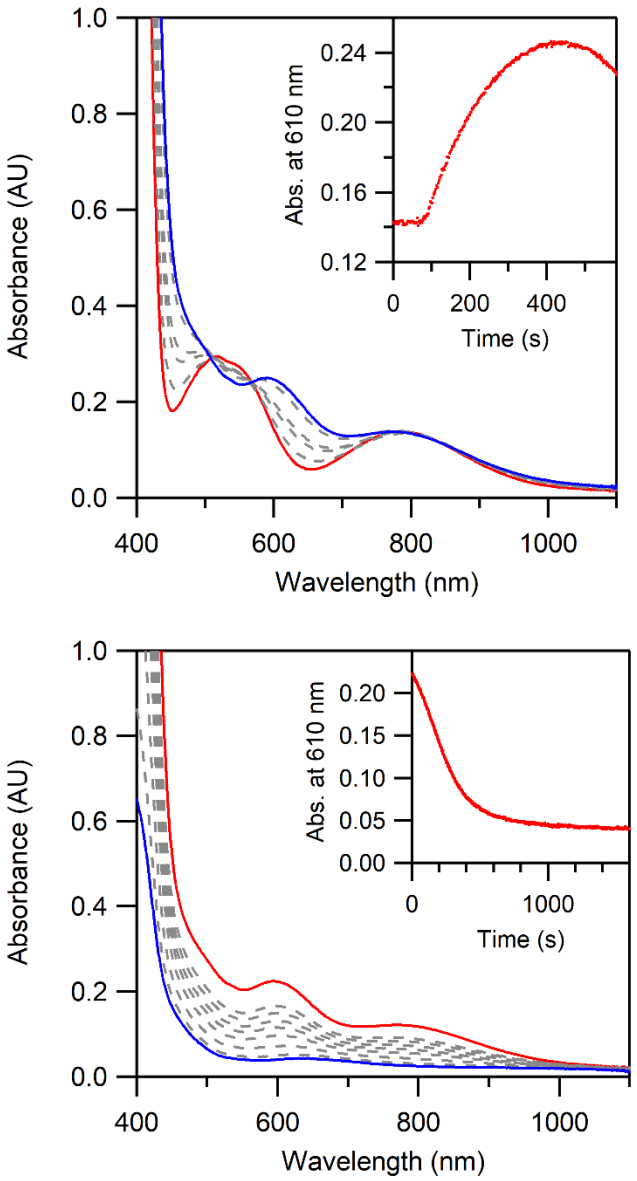

Figure S5. Top: Electronic absorption spectra of **3** (blue trace) after the addition of 5 equiv. H_2O_2 and 1 equiv. perchloric acid to a 1.25 mM solution of $[Mn^{III}(OH)(dpaq^{2Me})]^+$ in MeCN at -40°C (red trace). Inset: Time trace indicating the growth of the feature at 610 nm. Bottom: Electronic absorption spectra of the self-decay of **3** in MeCN at -40°C. Inset: Decay trace of the feature at 610 nm over time.

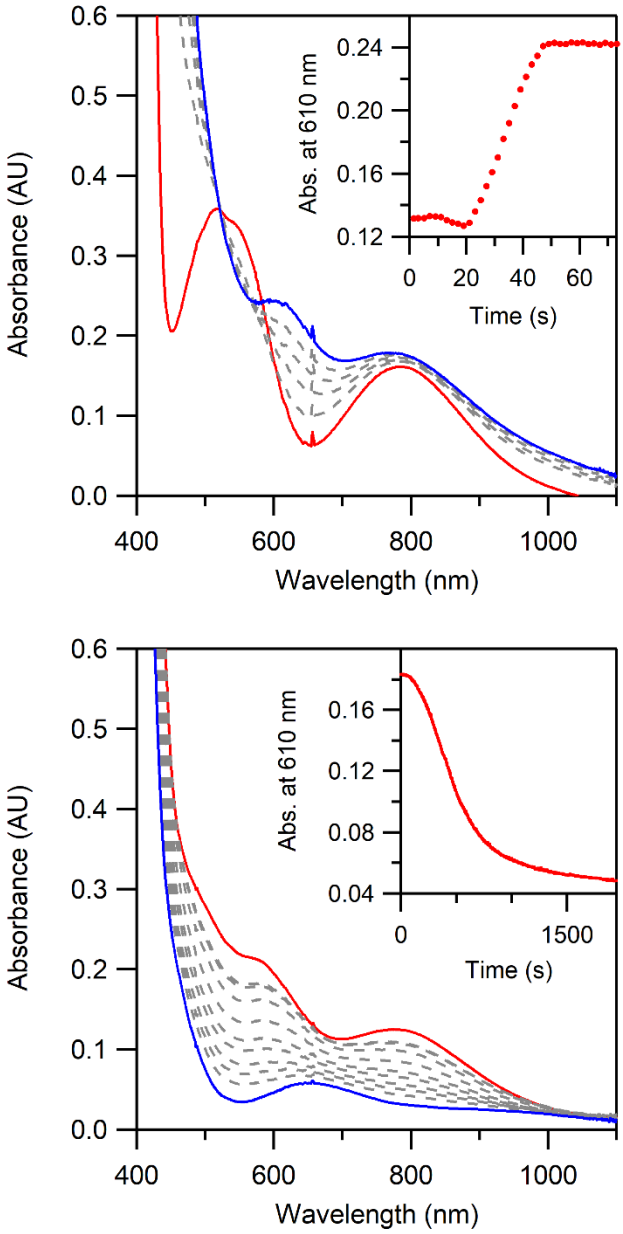

Figure S6. Top: Electronic absorption spectra of **3** (blue trace) formed after the addition of 5 equiv. H_2O_2 and 1 equiv. acetic acid to a 1.25 mM solution of $[Mn^{III}(OH)(dpaq^{2Me})]^+$ (red trace) in MeCN at -40°C. Inset: Time trace indicating the growth of the features at 610 nm. Bottom: Electronic absorption spectra of the self-decay of **3** (formed using acetic acid) in MeCN at -40°C. Inset: Decay trace of the feature at 610 nm over time.

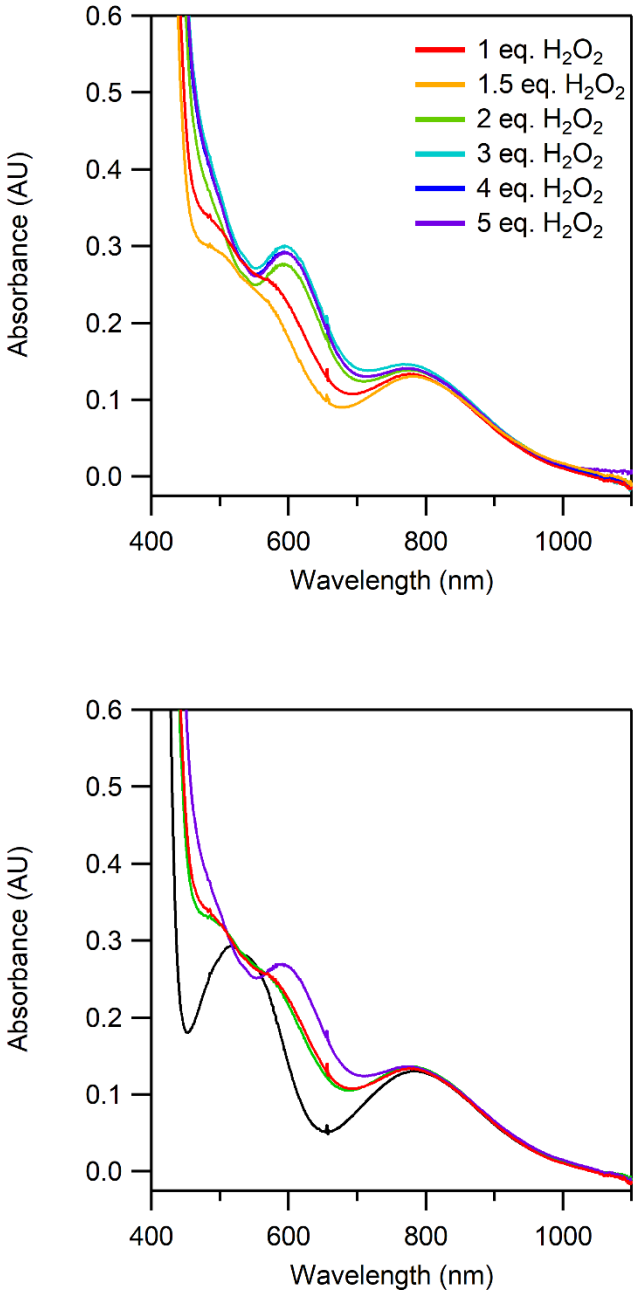

Figure S7. Top: Electronic absorption spectra for the addition of 1-5 equivalents of H_2O_2 and 0.1 equiv. $HClO_4$ to a 1.25 mM solution of $[Mn^{III}(OH)(dpaq^{2Me})]^+$ at -40°C. Bottom: Electronic absorption spectra for the addition of 1 equiv. H_2O_2 and 0.1 equiv. $HClO_4$ (red). This trace can be described as a linear combination of **1** (black trace), and **3** (purple trace). The linear combination that best reproduces the experimental spectrum requires a 0.46:0.54 ratio of **1**:**3** (green trace).

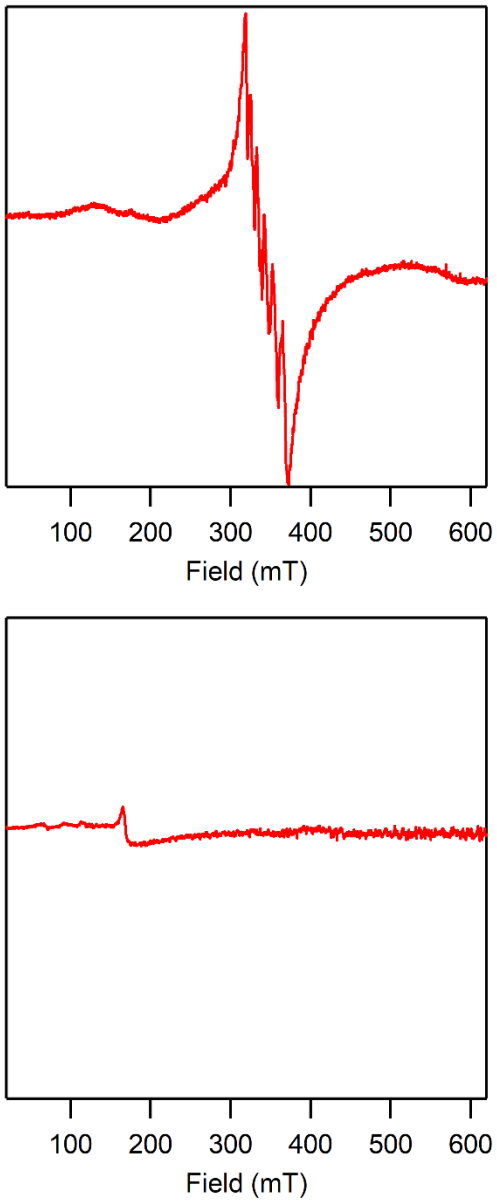

Figure S8. 7.5 K perpendicular-mode (top) and parallel-mode (bottom) EPR spectra of **3** obtained following the reaction of a 3 mM solution of $[Mn^{III}(OH)(dpaq^{2Me})]^{+}$ with 5 equiv. H_2O_2 and 0.1 equiv. $HClO_4$ in 1:1 MeCN:toluene at -40°C. The weak feature near 180 mT in the bottom spectrum is from O_2.

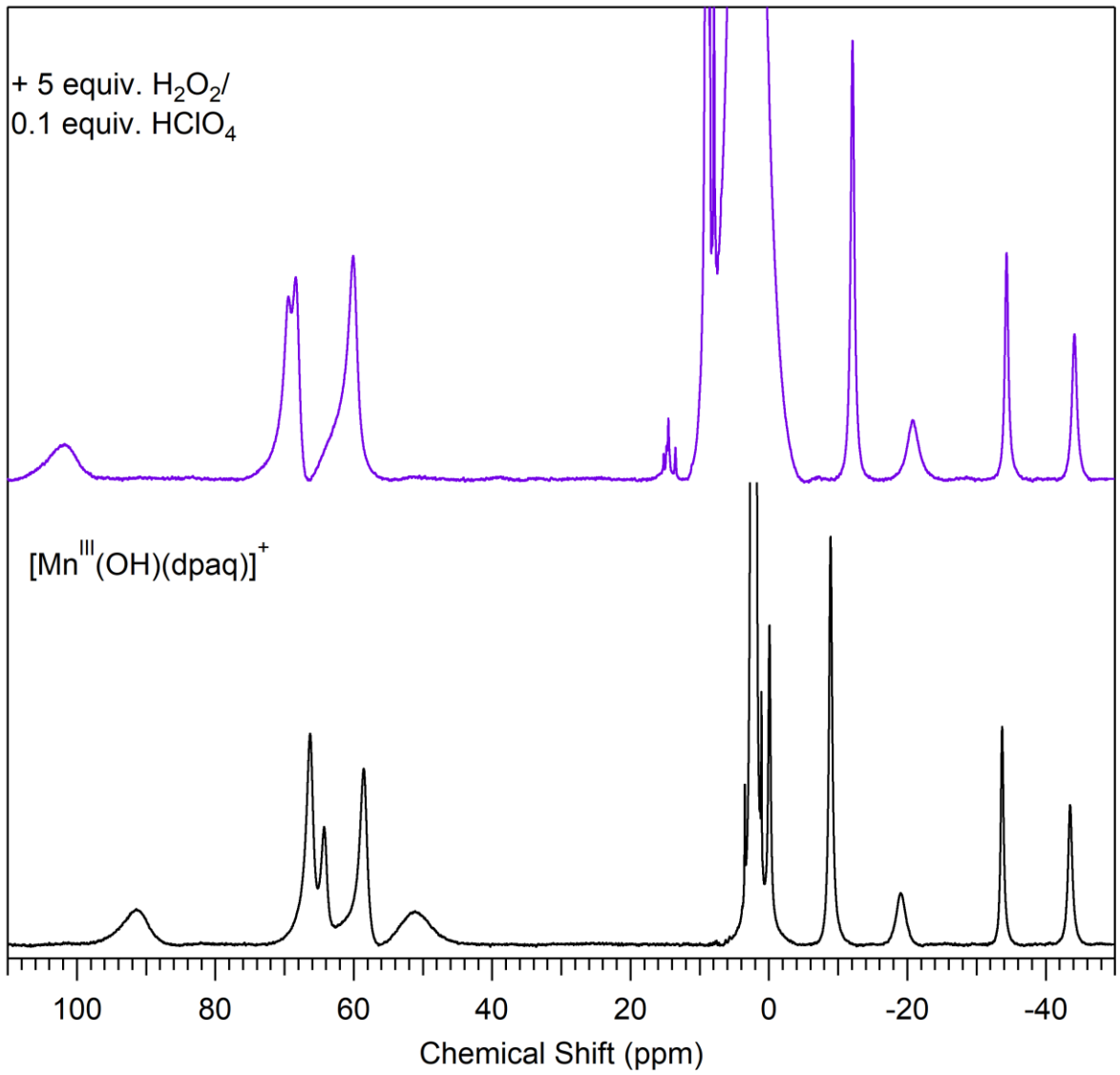
+ 5 equiv. H_2O_2/
0.1 equiv. $HClO_4$
$[Mn^{III}(OH)(dpaq)]^+$
100
80
60
40
20
0
-20
-40
Chemical Shift (ppm)

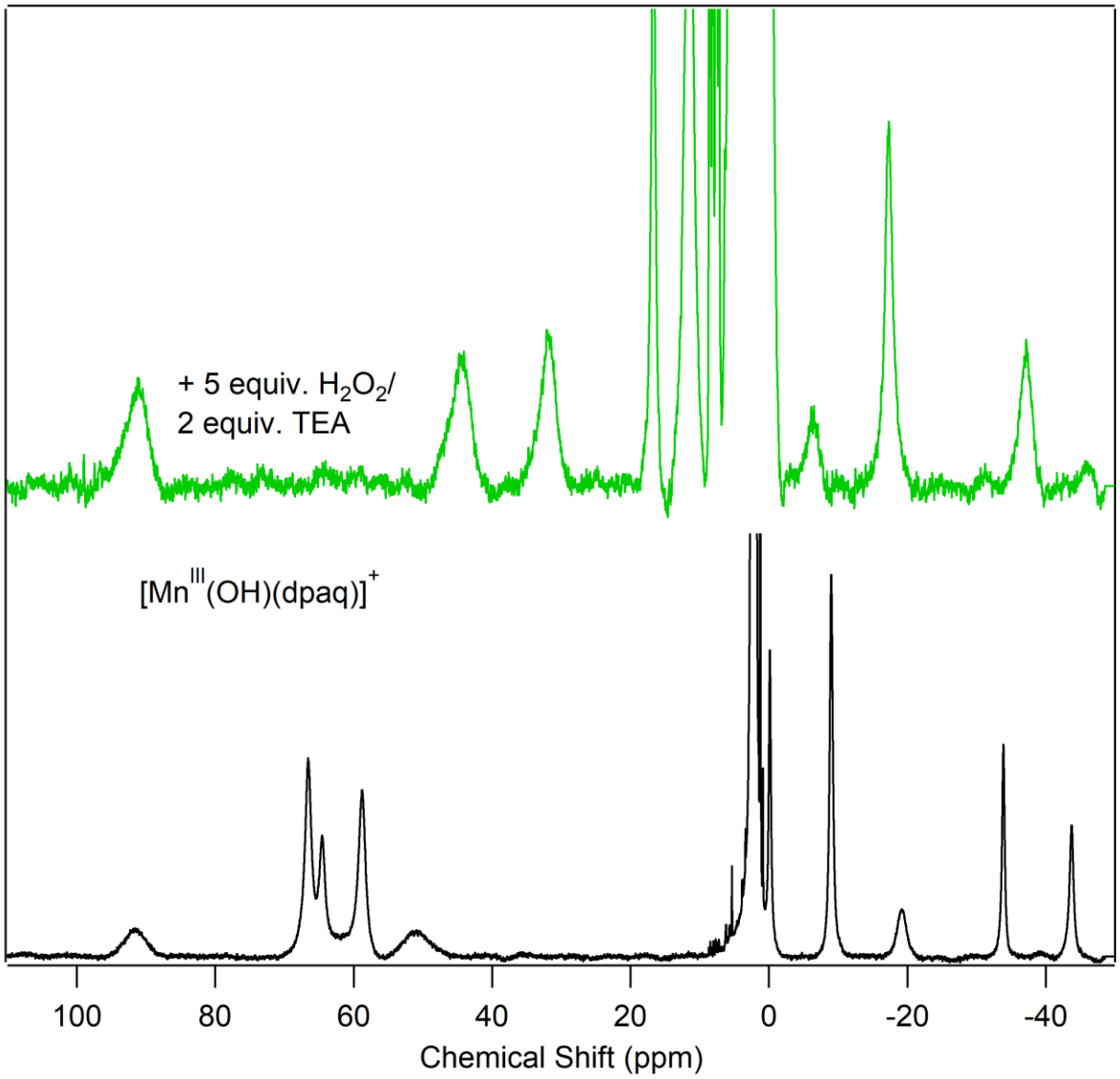
+ 5 equiv. H2O2/
2 equiv. TEA
[Mn^III(OH)(dpaq)]^+
100
80
60
40
20
0
-20
-40
Chemical Shift (ppm)

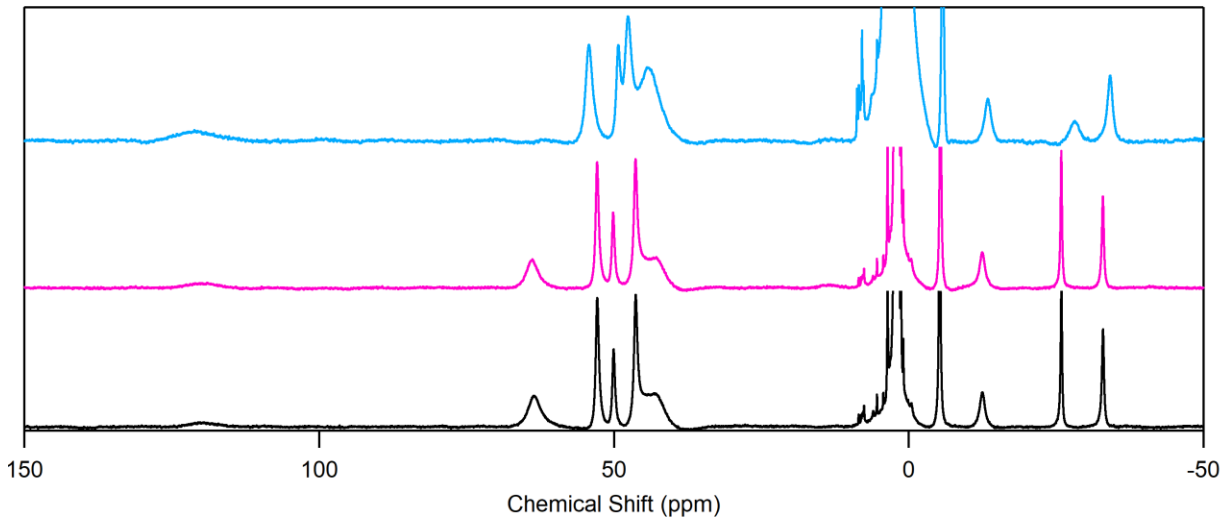

Figure S9. Top (page S9): Low temperature ^{1}H NMR spectra of 3 mM **1** (black trace) in *d3*-MeCN and a 3 mM solution of **3** formed with 5 equiv. H_2O_2 and 0.1 equiv. $HClO_4$ (purple trace) in *d3*-MeCN. **Center (page S10):** Expanded view of the Low temperature ^{1}H NMR spectra of 3 mM **1** (black trace) in *d3*-MeCN and a 3 mM solution of **4** formed with 10 equivalents each of H_2O_2 and Et_3N (green trace) in *d3*-MeCN. Spectra were collected at -40°C. **Bottom (page S11):** ^{1}H NMR spectra of 3 mM **1** (black trace, bottom) in *d3*-MeCN, a 3 mM solution of **1** in the presence of 10 equiv. D_2O in *d3*-MeCN (pink trace, middle) and a 3 mM solution of **1** in the presence of 10 equiv. D_2O and 0.2 equiv. $HClO_4$ in *d3*-MeCN (blue trace, top).

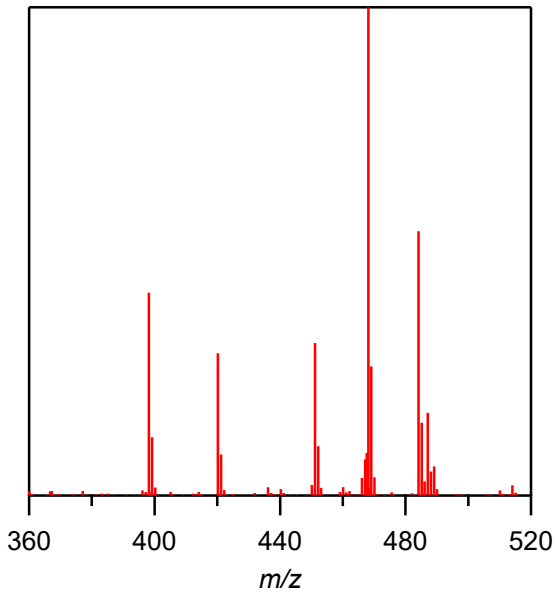

Figure S10. ESI-MS data for **3**. Peaks are assigned as follows: *m/z* = 484.1 $[Mn^{III}(OOH)(dpaq^{2Me})]^{+}$; *m/z* = 468.1 $[Mn^{III}(OH)(dpaq^{2Me})]^{+}$; *m/z* = 451.1 $[Mn^{II}(dpaq^{2Me})]^{+}$; *m/z* = 420.1 $Na^{+}dpaq^{2Me}H$; *m/z* = 398.2 $dpaq^{2Me}H_2^{+}$.

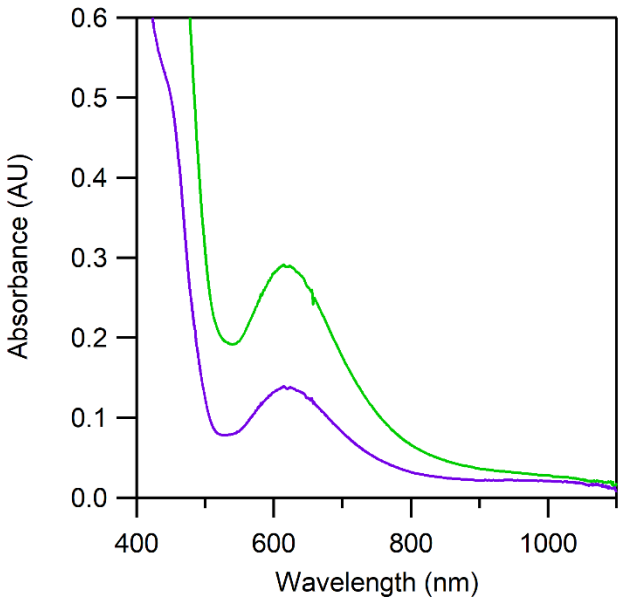

Figure S11. Overlay of electronic absorption spectra of **4** formed by the simultaneous addition of 5 equiv. H_2O_2 and 2 equiv. Et_3N (green trace) with the final spectrum of the reaction of **3** with 2 equiv. Et_3N (purple trace).

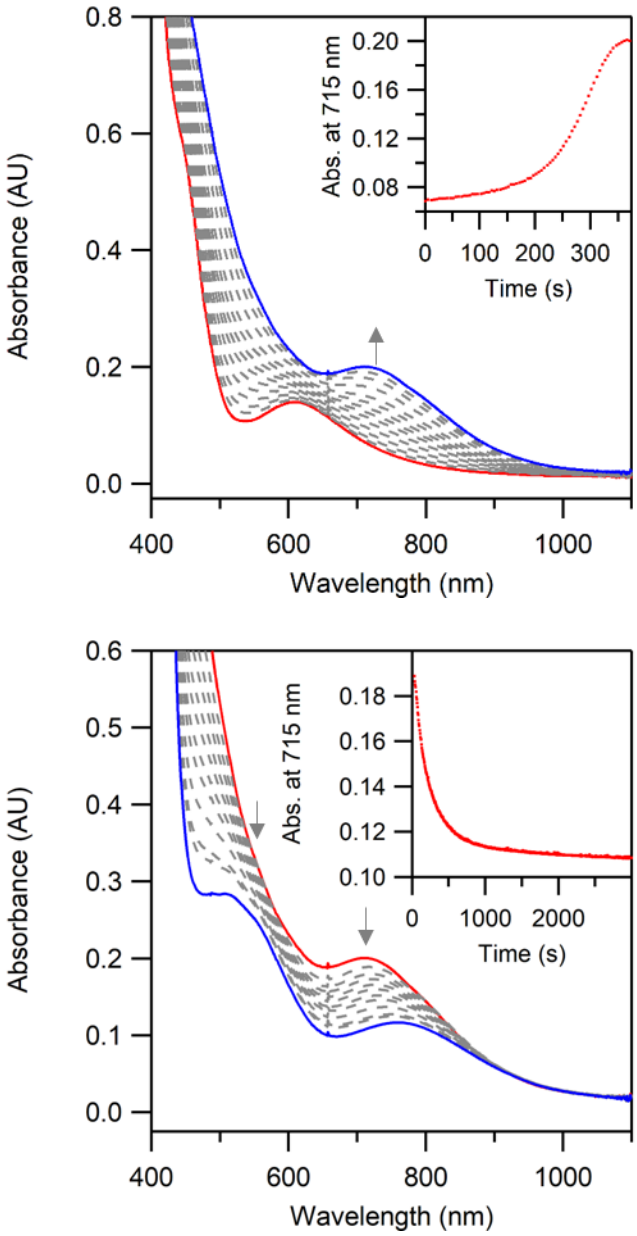

Figure S12. Top: Electronic absorption spectra for the self-decay of **4** (red trace) in MeCN to form **2** (blue trace) at 25°C. Inset: Time trace indicating the growth of the feature at 710 nm. Bottom: Electronic absorption spectra of the self-decay of **2** formed from the initial decay of **4** (red trace) in MeCN to form **1** (blue trace) at 25°C. Inset: Decay trace of the feature at 710 nm over time.

Table S2. Compositions and energies of α-spin MOs for $[Mn^{III}(OH)(dpaq^{2Me})]^+$ (**1**) from DFT Computations

Orbital	**105a**	**108a**	**113a**	**114a**	**120a**	**121a**	**123a**
	dxz (α)	dxy (α)	dxy/yz (α)	dxy (α)	dxz (α)	dx^2-y^2 (α)	dz^2 (α)
Energy (eV)	-9.105	-8.707	-7.663	-6.194	-6.366	-5.349	-2.646
Occ.	1	1	1	1	1	1	0
LÖWDIN REDUCED ORBITAL POPULATIONS PER MO							
	0	0.4	1.1	0.2	0	0.9	50.3
xz	21.2	0.4	0.6	0	17.3	0.6	1.2
yz	3.2	6.6	16.4	0.8	0.2	0.1	0
x^2-y^2	0	0.1	0	0	0	46.8	0.6
xy	2.3	22.6	19.2	16.8	0	0	0.1
p_z (O)	0.5	1	9.8	1.3	0.1	0.4	8.7
p_x (O)	5.5	0.1	3.4	0.3	27.4	0.3	0.1
p_y (O)	0.9	0.1	6.4	1.4	0.5	0.1	0.3
p_z (N_{amide})	0.0	0.9	1.8	0.0	0.5	0.0	5.7
p_x (N_{amide})	0.0	0.0	0.0	0.0	1.7	0.0	0.1
p_y (N_{amide})	0.0	0.1	2.5	6.8	0.0	0.0	0.1
	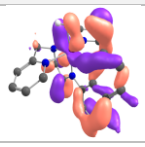		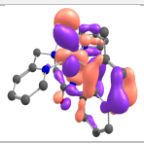	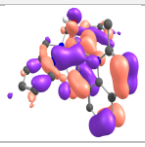	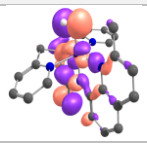	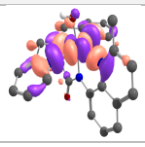	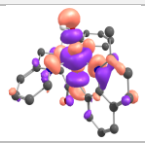

Table S3. Compositions and energies of β-spin MOs for $[Mn^{III}(OH)(dpaq^{2Me})]^{+}$ (**1**) from DFT Computations

Orbital	**119b**	**120b**	**122b**	**123b**	**124b**	**128b**	**129b**
	dxy (β)	dyz (β)	dxz (β)	dxz/xy (β)	dyz (β)	dx^2-y^2 (β)	dz^2 (β)
Energy (eV)	-2.687	-2.321	-1.993	-1.790	-1.427	-0.718	-0.686
Occ.	0	0	0	0	0	0	0
LÖWDIN REDUCED ORBITAL POPULATIONS PER MO							
z^2	0	0	0.6	0.2	0.6	0.1	63.2
xz	0	0.8	37.1	29.4	0.1	2.1	1.3
yz	5.6	33.6	3	10.2	20.5	0.6	0.7
x^2-y^2	0	0.2	1.1	0.8	0.6	68.3	0
xy	21.3	13.3	17.5	17.3	10.1	0.2	0.1
p_z (O)	0	0.5	0	0.1	0	0	5.3
p_x (O)	0.1	0	3.4	3.0	0	0.3	0
p_y (O)	0	1.4	0	0.3	0.2	0	0.1
p_z (N_{amide})	0.0	0.0	0.0	0.0	0.0	0.1	3.1
p_x (N_{amide})	0.0	0.7	0.0	0.2	0.0	0.0	0.0
p_y (N_{amide})	0.0	0.0	0.0	0.0	0.0	0.0	0.4
	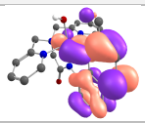	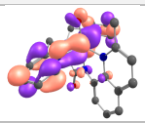	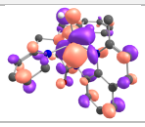	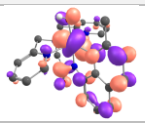	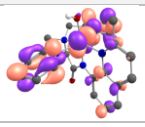	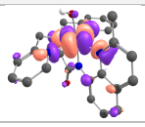	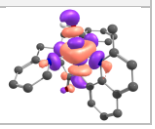

Table S4. Compositions and energies of α-spin MOs for $[Mn^{III}(OOH)(dpaq^{2Me})]^{+}$ (**3**) from DFT Computations

Orbital	**113a**	**116a**	**117a**	**123a**	**125a**	**127a**
	dyz	dyz	dxy	dxz	dx^2-y^2	dz^2
Energy (eV)	-8.422	-7.899	-7.534	-6.417	-5.486	-2.820
Occ.	1	1	1	1	1	0
LÖWDIN REDUCED ORBITAL POPULATIONS PER MO						
dz^2	0.3	0.1	0.6	0.9	0.3	50.4
dxz	3.6	0.5	0.2	12.3	0.3	1.0
dyz	19.9	13.7	2.2	1.8	0.0	0.0
dx^2-y^2	0.0	0.7	0.5	0.2	42.2	0.2
dxy	2.8	1.1	26.6	0.3	0.9	0.0
p_z (O_{prox})	1.3	0.1	1.6	7.3	0.3	11.9
p_x (O_{prox})	2.0	0.3	0.1	18.4	0.1	0.3
p_y (O_{prox})	0.6	0.2	0.5	15.5	0.1	0.6
p_z (O_{dist})	1.4	0.0	1.1	15.7	0.2	2.0
p_x (O_{dist})	3.5	0.0	0.0	2.9	0.0	0
p_y (O_{dist})	0.3	0.5	0.4	3.9	0.0	0
p_z (N_{amide})	0.1	0.1	0.1	1.4	0.0	5.8
p_x (N_{amide})	0.0	0.0	0.0	0.0	0.1	0.1
p_y (N_{amide})	0.2	0.2	3.3	0.5	0.9	0.1
	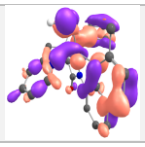	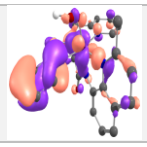	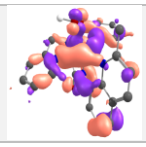	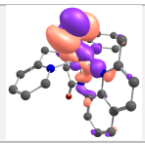	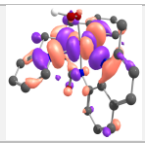	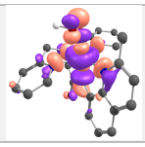

Table S5. Compositions and energies of β-spin MOs for $[Mn^{III}(OOH)(dpaq^{2Me})]^{+}$ (**3**) from DFT Computations

Orbital	**125b**	**126b**	**127b**	**128b**	**132b**	**133b**
	dxz	dxy	dxz/xy	dyz	dx^2-y^2	dz^2
Energy (eV)	-2.241	-2.028	-1.808	-1.489	-0.896	-0.808
Occ.	0	0	0	0	0	0
LÖWDIN REDUCED ORBITAL POPULATIONS PER MO						
dz^2	0.9	0.5	0.1	0.9	6.6	56.7
dxz	37.3	0	23.7	0.7	2.8	0.5
dyz	1.5	1.1	5.8	19.2	0.7	1.8
dx_2-y_2	1.5	1.2	0.1	2.9	58	6.8
dxy	18.3	7.8	17.7	7.6	0.1	0.7
p_z (O_{prox})	0	0.1	0	0	0.6	5.4
p_x (O_{prox})	2.3	0	1.7	0.6	0.3	0.1
p_y (O_{prox})	2.4	0.1	0.6	0	0	0.3
p_z (O_{dist})	0.1	0	0.2	0.3	0	0.7
p_x (O_{dist})	0.4	0.1	0.1	0.2	0	0.1
p_y (O_{dist})	0.2	0	0	0	0	0
p_z (N_{amide})	0.0	0.0	0.0	0.0	0.5	2.7
p_x (N_{amide})	0.1	0.0	0.0	0.0	0.0	0.1
p_y (N_{amide})	0.1	0.0	0.2	0.1	0.1	0.3
	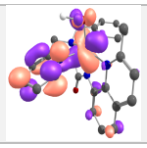	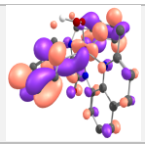	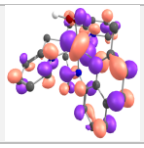	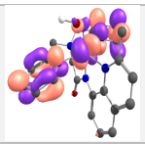	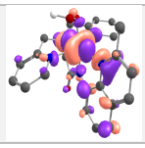	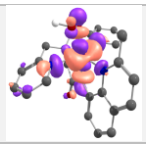

Table S6. Electronic Transitions for $[Mn^{III}(OH)(dpaq^{2Me})]^{+}$ (**1**) from TD-DFT Computations

State	Wavelength	f_{osc}	transition	%	donor identity	acceptor identity		EDDM
1	778.6	0.000887	121a⟶123a	88.8	x^2-y^2	z^2	x^2-y^2⟶z^2	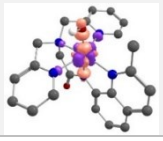
2	535.7	0.001237	122a⟶123a	67.0	yz	z^2	yz⟶z^2	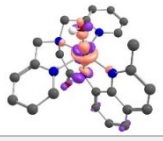
3	501.6	0.000267	122a⟶124a 118b⟶119 b	40.5 49.4	qn qn	qn qn/xy	N⟶xy/qn	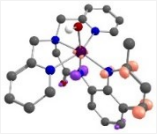
4	483.5	0.00321	118a⟶123a 120a⟶123a	25.6 35.8	O/xz O/xz	z^2 z^2	xz⟶z^2	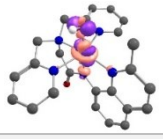
5	401.7	0.043872	112a⟶124a 118b⟶119 b	34.2 42.2	x^2-y^2 qn/N	qn qn/xy	N⟶xy	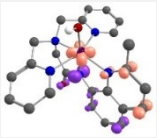
6	386.6	0.001621	121a⟶124a	94.4	x^2-y^2	qn	x^2-y^2⟶qn	
7	381.9	0.020894	118b⟶120 b	86.8	N/qn	xy/yz	N⟶yz	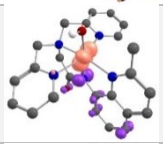
8	380.2	0.004355	114a⟶123a 115a⟶123a	23.2 21.6	py/yz qn/xz/ O	z^2 z^2	yz⟶z^2	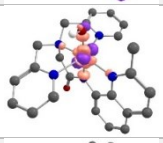
9	356.1	0.018858	118b⟶122 b	36.6	qn	O/xz	N⟶xz	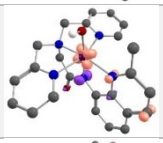
10	353.6	0.002423	121a⟶125a	83.4	x^2-y^2	py	x^2-y^2⟶py	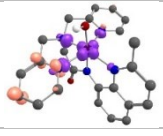

Table S7. Electronic Transitions for $[Mn^{III}(OOH)(dpaq^{2Me})]^{+}$ (**3**) from TD-DFT Computations

State	Wavelength	f_{osc}	transition	%	donor identity	acceptor identity		EDDM
1	771.4	0.001186	125a⟶127a	89.2	x^2-y^2	z^2	x^2-y^2⟶z^2	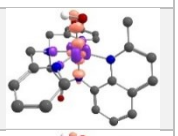
2	579.2	0.002166	126a⟶127a	69.6	yz	z^2	xz/yz⟶z^2	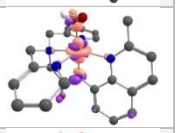
3	491.6	0.000376	126a⟶128a 122b⟶123b	40.3 44.5	qn qn	qn qn/xy/yz	N⟶xy/qn	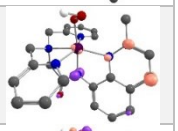
4	472.4	0.004367	123a⟶127a 126a⟶127a	39.6 22.1	xz	z^2 z^2	xz⟶z^2	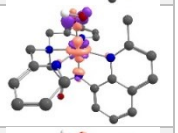
5	420.2	0.011464	122b⟶124b	58.9	qn	xz/yz	N⟶xz/yz	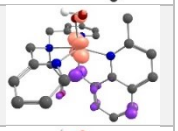
6	397.4	0.023143	126a⟶129a 122b⟶123b 122b⟶124b	23.1 17.5 27.5	qn/N qn/N qn/N	py qn/xy/yz xz/yz	N⟶x^2-y^2	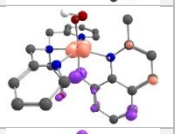
7	383.1	0.010565	117a⟶127a	24.1	xy/yz	z^2	xy/xz⟶z^2	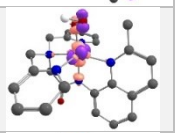
8	376.3	0.026596	122b⟶125b	70.4	qn/N	xz/yz	N⟶xz/yz	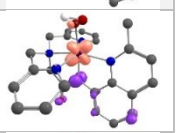
9	365.5	0.005251	125a⟶128a	90.4	x^2-y^2	qn	x^2-y^2⟶qn	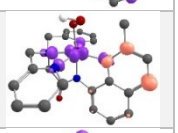
10	363.8	0.023259	124a⟶127a	35.7	O/xz	z^2	O⟶z^2	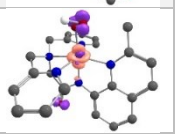

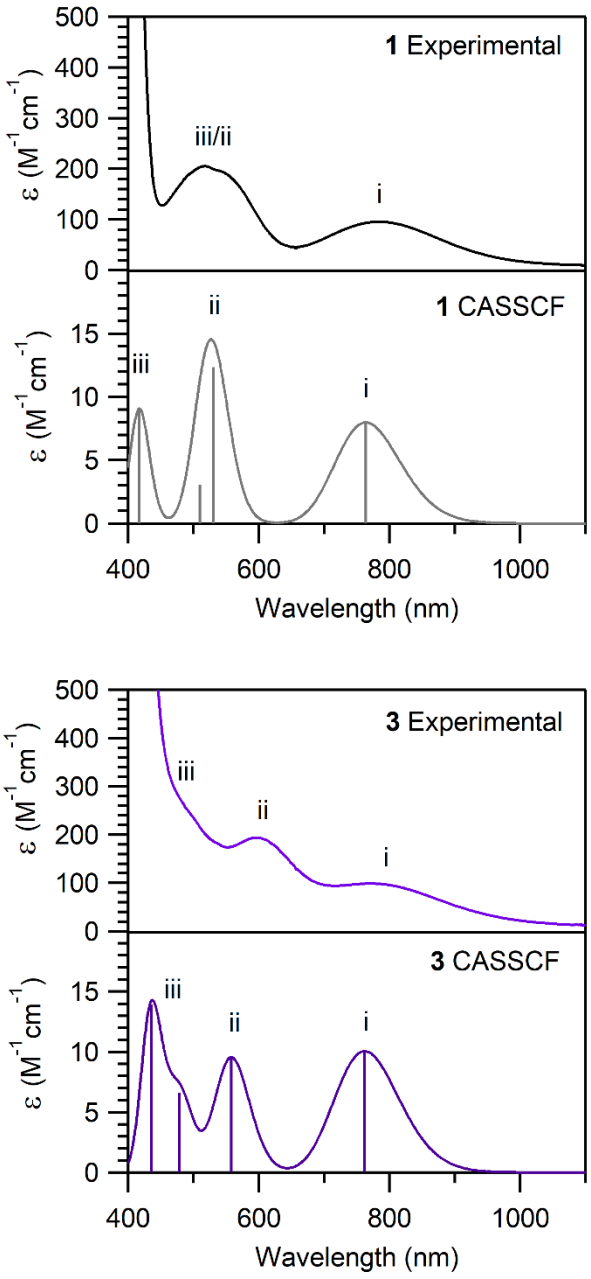

Figure S13. Experimental and CASSCF/NEVPT2 calculated UV-vis spectra for **1** (top) and **3** (bottom).

Table S8. Electronic Transitions for $[Mn^{III}(OH)(dpaq^{2Me})]^+$ (**1**) from CASSCF/NEVPT2 computations

Root	Wavelength	fosc	%	donor identity	acceptor identity
1	667.4	8.41E-05	78.3 20.9	x^2-y^2 xy	z^2
2	436.6	0.000138	45.2 29.0 18.0	xz yz xy	z^2
3	415.4	3.43E-05	53.4 35.2	xz yz	z^2
4	340.7	0.000102	53.4 35.0 10.1	xy yz x^2-y^2	z^2

Table S9. Electronic transitions for $[Mn^{III}(OOH)(dpaq^{2Me})]^+$ (**3**) from CASSCF/NEVPT2 computations

Root	Wavelength	fosc	%	donor identity	acceptor identity
1	646.0	0.000109	67.1 20.8	x^2-y^2 xy/xz	z^2
2	454.6	0.000108	86.1	yz	z^2
3	379.0	7.72E-05	48.1 42.7	xy/xz xz/xy	z^2
4	350.5	0.000159	39.0 33.6 26.5	xy/xz xz/xy x^2-y^2	z^2 z^2 z^2

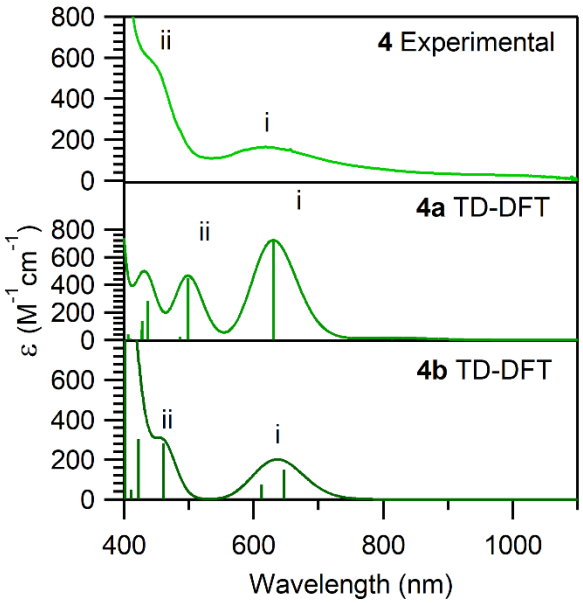

Figure S14. Experimental (top) and TD-DFT computed UV-vis spectra for the structure of **4a** (middle) and **4b** (bottom).

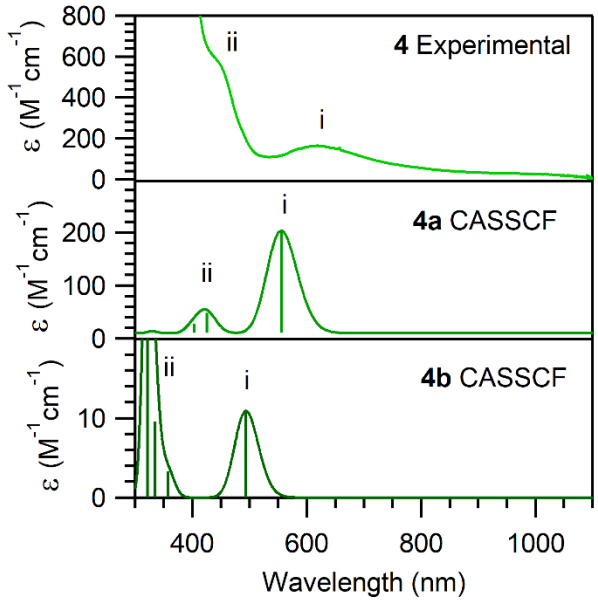

Figure S15. Experimental (top) and CASSCF/NEVPT2 calculated UV-vis spectra for **4a** (middle) and **4b** (bottom).

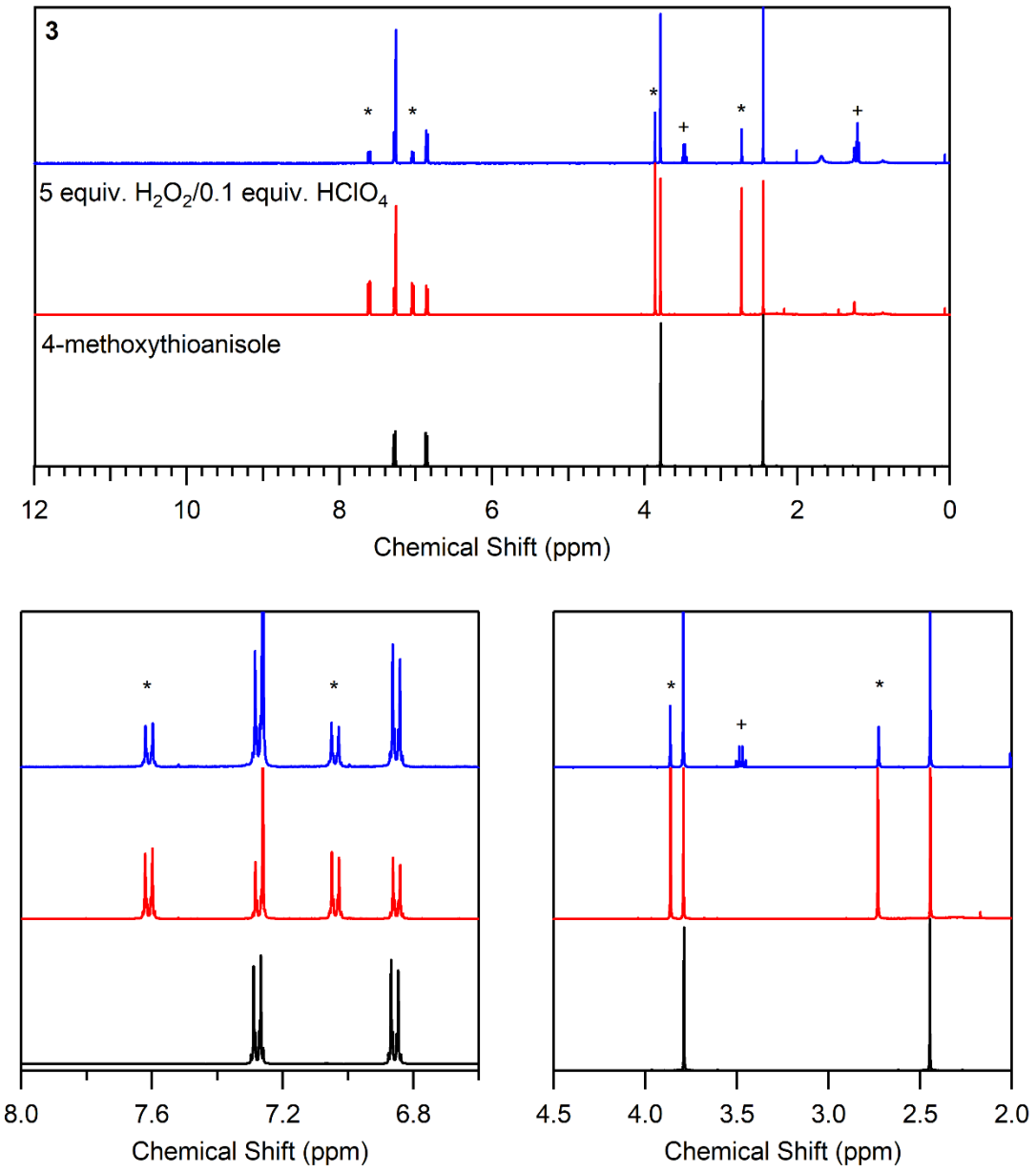

Figure S16. Top: ^{1}H NMR spectra for the organic products resulting from the reactions of a 1.25 mM solution of **3**, formed by the addition of 5 equiv. H_2O_2 and 0.1 equiv. $HClO_4$, with 5 equiv. 4-methoxythioanisole (blue trace), and the reaction of 4-methoxyanisole with H_2O_2 and $HClO_4$ in the absence of **3** (red trace). The ^{1}H NMR spectrum of 4-methoxyanisole is included for comparison (black trace). Bottom: Expanded region from 8 – 6.5 ppm (left) and 4.5 – 2 ppm (right). Legend: + ethanol; * 1-methoxy-4-(methylsulfinyl)benzene.

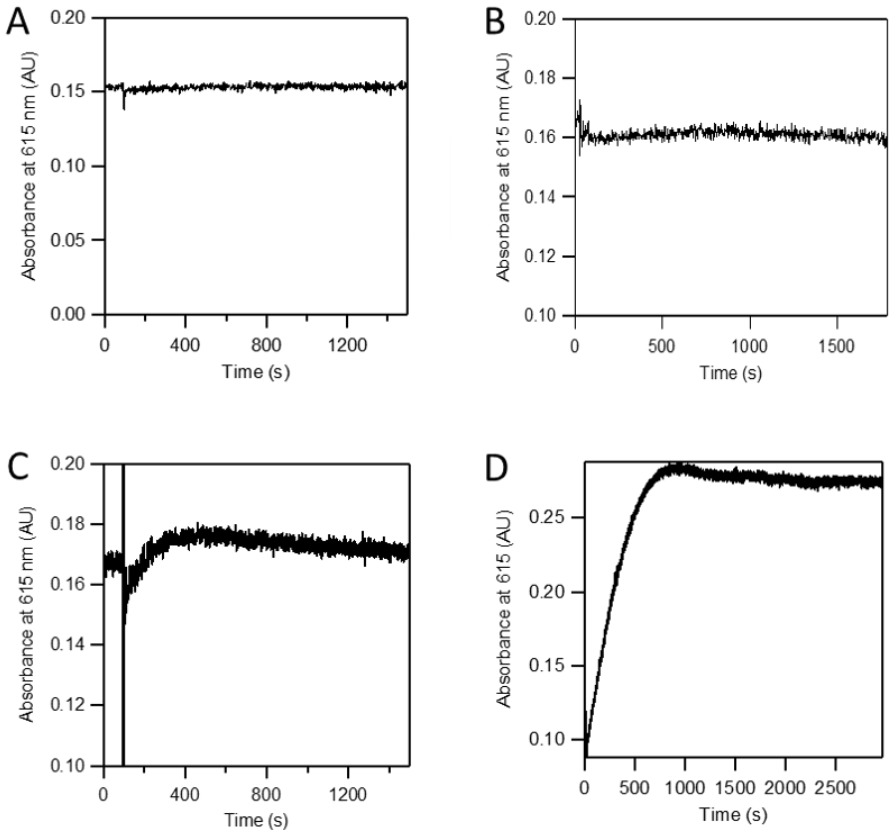

Figure S17. Time traces for the reactions of **4** with 100 equiv. of various substrates. There are no spectral changes after the addition of DHA (panel A), CHD (panel B), or 2,4,6-tri-*tert*-butylphenol (panel C) indicating that no reaction takes place with these substrates. The addition of 100 equivalents of TEMPOH results the formation of a precipitate (panel D).

Cartesian Coordinates from DFT optimized structures. All calculations were performed for S = 2 systems.

$[Mn^{III}(OH)(dpaq^{2Me})]^{+}$

25	0.000000000	0.000000000	0.000000000
8	1.756000000	0.387000000	-3.667000000
8	0.000000000	0.000000000	1.835000000
1	-0.150000000	0.874000000	2.237000000
7	-2.039000000	0.000000000	-0.549000000
7	0.209000000	0.080000000	-1.945000000
7	2.208000000	-0.054000000	-0.080000000
7	0.516000000	2.158000000	-0.091000000
7	0.498000000	-2.153000000	0.037000000
6	-3.137000000	-0.131000000	0.218000000
6	-4.431000000	0.024000000	-0.347000000
1	-5.302000000	-0.091000000	0.304000000
6	-4.584000000	0.313000000	-1.690000000
1	-5.582000000	0.440000000	-2.123000000
6	-3.442000000	0.432000000	-2.524000000
6	-3.505000000	0.702000000	-3.919000000
1	-4.481000000	0.844000000	-4.393000000
6	-2.331000000	0.775000000	-4.652000000
1	-2.371000000	0.981000000	-5.726000000
6	-1.063000000	0.580000000	-4.050000000
1	-0.153000000	0.631000000	-4.647000000
6	-0.962000000	0.314000000	-2.678000000
6	-2.165000000	0.252000000	-1.904000000
6	1.469000000	0.140000000	-2.497000000
6	2.587000000	-0.225000000	-1.512000000
1	2.826000000	-1.288000000	-1.687000000
1	3.487000000	0.360000000	-1.760000000
6	2.674000000	1.237000000	0.485000000
1	3.748000000	1.399000000	0.285000000
1	2.525000000	1.179000000	1.576000000
6	1.847000000	2.383000000	-0.057000000
6	2.392000000	3.602000000	-0.469000000
1	3.475000000	3.755000000	-0.442000000
6	1.531000000	4.613000000	-0.919000000
1	1.934000000	5.574000000	-1.253000000
6	0.152000000	4.370000000	-0.944000000
1	-0.553000000	5.130000000	-1.291000000
6	-0.314000000	3.121000000	-0.525000000
1	-1.379000000	2.870000000	-0.542000000

6	2.603000000	-1.210000000	0.764000000
1	3.683000000	-1.431000000	0.677000000
1	2.375000000	-0.938000000	1.808000000
6	1.772000000	-2.419000000	0.389000000
6	2.260000000	-3.730000000	0.424000000
1	3.301000000	-3.921000000	0.702000000
6	1.395000000	-4.783000000	0.098000000
1	1.752000000	-5.817000000	0.119000000
6	0.073000000	-4.493000000	-0.265000000
1	-0.630000000	-5.285000000	-0.534000000
6	-0.333000000	-3.156000000	-0.287000000
1	-1.348000000	-2.866000000	-0.576000000
6	-2.993000000	-0.434000000	1.683000000
1	-2.144000000	-1.103000000	1.881000000
1	-2.803000000	0.495000000	2.251000000
1	-3.923000000	-0.877000000	2.071000000

$[Mn^{III}(OOH)(dpaq^{2Me})]^{+}$

25	0.000000000	0.000000000	0.000000000
8	1.772000000	0.278000000	-3.676000000
8	0.000000000	0.000000000	1.856000000
7	-2.045000000	0.000000000	-0.572000000
7	0.208000000	0.058000000	-1.955000000
7	2.227000000	-0.261000000	-0.112000000
7	0.738000000	2.070000000	-0.134000000
7	0.341000000	-2.183000000	0.106000000
6	-3.151000000	-0.159000000	0.173000000
6	-4.431000000	0.149000000	-0.367000000
1	-5.311000000	0.015000000	0.268000000
6	-4.556000000	0.606000000	-1.664000000
1	-5.540000000	0.853000000	-2.077000000
6	-3.402000000	0.735000000	-2.486000000
6	-3.438000000	1.155000000	-3.844000000
1	-4.398000000	1.418000000	-4.298000000
6	-2.258000000	1.214000000	-4.569000000
1	-2.278000000	1.533000000	-5.616000000
6	-1.011000000	0.861000000	-3.997000000
1	-0.098000000	0.898000000	-4.590000000
6	-0.937000000	0.450000000	-2.659000000
6	-2.146000000	0.401000000	-1.893000000
6	1.464000000	0.017000000	-2.513000000
6	2.540000000	-0.504000000	-1.550000000
1	2.606000000	-1.593000000	-1.711000000
1	3.513000000	-0.066000000	-1.826000000

6	2.831000000	0.994000000	0.393000000
1	3.906000000	1.056000000	0.142000000
1	2.734000000	0.980000000	1.492000000
6	2.082000000	2.194000000	-0.144000000
6	2.704000000	3.367000000	-0.581000000
1	3.796000000	3.439000000	-0.587000000
6	1.906000000	4.436000000	-1.012000000
6	0.512000000	4.299000000	-0.989000000
1	-0.145000000	5.108000000	-1.317000000
6	-0.033000000	3.091000000	-0.544000000
1	-1.114000000	2.922000000	-0.513000000
6	2.546000000	-1.427000000	0.748000000
1	3.597000000	-1.751000000	0.632000000
1	2.394000000	-1.113000000	1.795000000
6	1.595000000	-2.560000000	0.430000000
6	1.961000000	-3.910000000	0.481000000
1	2.987000000	-4.190000000	0.737000000
6	0.994000000	-4.884000000	0.199000000
6	-0.304000000	-4.479000000	-0.139000000
1	-1.084000000	-5.207000000	-0.377000000
6	-0.587000000	-3.111000000	-0.179000000
1	-1.576000000	-2.733000000	-0.450000000
6	-3.042000000	-0.687000000	1.575000000
1	-2.044000000	-1.096000000	1.781000000
1	-3.227000000	0.121000000	2.304000000
1	-3.809000000	-1.463000000	1.740000000
1	2.368000000	5.361000000	-1.368000000
1	1.254000000	-5.946000000	0.232000000
8	-0.792000000	1.171000000	2.242000000
1	-0.088000000	1.782000000	2.543000000

[Mn^{III}(O2)($dpaq^{2Me}$)] – Quinoline Bound

25	1.970982000	7.777498000	7.952709000
8	3.859555000	4.041205000	7.688540000
8	1.563145000	9.450207000	7.316355000
7	1.289760000	7.285535000	10.272560000
7	2.810825000	5.957684000	8.535370000
7	2.413093000	6.922226000	5.954879000
7	4.341472000	8.134369000	7.576013000
7	0.078183000	6.717104000	7.251789000
6	0.490287000	7.990768000	11.070828000
6	0.626988000	7.935473000	12.489976000
1	-0.050076000	8.525115000	13.116022000
6	1.607216000	7.143578000	13.055905000

1	1.729867000	7.093521000	14.143381000
6	2.471962000	6.380069000	12.219854000
6	3.506852000	5.537160000	12.714940000
1	3.665158000	5.457095000	13.795595000
6	4.296635000	4.834012000	11.815588000
1	5.099540000	4.187228000	12.187188000
6	4.096706000	4.927865000	10.415908000
1	4.731482000	4.361925000	9.734182000
6	3.089642000	5.746719000	9.881928000
6	2.262856000	6.487569000	10.805828000
6	3.228806000	5.112193000	7.560823000
6	2.750267000	5.482982000	6.150566000
1	1.842318000	4.884960000	5.966236000
1	3.505062000	5.158508000	5.414529000
6	3.551277000	7.668344000	5.356047000
1	3.870631000	7.201011000	4.407591000
1	3.191575000	8.687750000	5.140801000
6	4.697206000	7.748284000	6.335504000
6	6.025562000	7.458674000	5.998707000
1	6.279522000	7.138019000	4.983929000
6	7.011721000	7.586466000	6.987544000
1	8.058432000	7.364547000	6.756574000
6	6.635892000	7.994391000	8.273768000
1	7.373838000	8.105101000	9.073761000
6	5.282158000	8.255418000	8.522102000
1	4.935072000	8.568806000	9.512340000
6	1.185607000	7.100510000	5.140110000
1	1.266546000	6.593358000	4.161761000
1	1.068021000	8.181667000	4.953861000
6	-0.004745000	6.581867000	5.911966000
6	-1.112423000	5.985504000	5.296892000
1	-1.142338000	5.880631000	4.208482000
6	-2.161914000	5.521311000	6.099788000
1	-3.040492000	5.052837000	5.645522000
6	-2.058277000	5.646057000	7.491655000
1	-2.844090000	5.277845000	8.157211000
6	-0.914483000	6.246734000	8.025026000
1	-0.768863000	6.351099000	9.102767000
6	-0.586592000	8.834813000	10.443073000
1	-0.463706000	8.870650000	9.351642000
1	-0.549381000	9.866014000	10.835476000
1	-1.585333000	8.429120000	10.691663000
8	1.931068000	9.546970000	8.708875000

[Mn^{III}(O2)($dpaq^{2Me}$)] – Quinoline Dissociated

25	2.426424000	7.553832000	8.099344000
8	5.083487000	4.450649000	8.496531000
8	1.409163000	9.092518000	7.976327000
7	2.512734000	3.456709000	9.450504000
7	3.436862000	6.049485000	8.928314000
7	3.013618000	6.491046000	6.217275000
7	4.249553000	8.636073000	7.247770000
7	0.798342000	6.036799000	7.843569000
6	2.092124000	2.220755000	9.671907000
6	1.728201000	1.760592000	10.974741000
1	1.386405000	0.728986000	11.112292000
6	1.805480000	2.630903000	12.043006000
1	1.516520000	2.313205000	13.051603000
6	2.270417000	3.961807000	11.840169000
6	2.356098000	4.922767000	12.884987000
1	2.065632000	4.636162000	13.901722000
6	2.794974000	6.207716000	12.601134000
1	2.852557000	6.957163000	13.397645000
6	3.181432000	6.567992000	11.289304000
1	3.523294000	7.585347000	11.077311000
6	3.136518000	5.650913000	10.237619000
6	2.642562000	4.320215000	10.497529000
6	4.250455000	5.288351000	8.141942000
6	4.135505000	5.581634000	6.635343000
1	4.042323000	4.610618000	6.119279000
1	5.087462000	6.032435000	6.312192000
6	3.488082000	7.511034000	5.253468000
1	3.954221000	7.051972000	4.358764000
1	2.607630000	8.087851000	4.917108000
6	4.457544000	8.458955000	5.931589000
6	5.471784000	9.139199000	5.246624000
1	5.631899000	8.962179000	4.178228000
6	6.270577000	10.044443000	5.958175000
1	7.071234000	10.591797000	5.450576000
6	6.033939000	10.233695000	7.326173000
6	5.010384000	9.499730000	7.934762000
1	4.774566000	9.595808000	8.999052000
6	1.839516000	5.749843000	5.691296000
1	2.150625000	4.944419000	4.998860000
1	1.232689000	6.472705000	5.118161000

6	0.973850000	5.198287000	6.805637000
6	0.337621000	3.955848000	6.744877000
1	0.499633000	3.294645000	5.887911000
6	-0.499643000	3.577164000	7.803680000
1	-1.003654000	2.605932000	7.788846000
6	-0.663279000	4.447983000	8.886538000
1	-1.292685000	4.181985000	9.740230000
6	0.011106000	5.673463000	8.867890000
1	-0.066016000	6.395361000	9.686946000
6	2.032110000	1.285347000	8.487529000
1	2.246747000	1.843471000	7.564511000
1	1.045523000	0.793894000	8.403180000
1	2.786591000	0.483759000	8.593868000
8	1.854737000	8.806329000	9.323914000
1	6.636678000	10.930629000	7.915563000

References

1. Rice, D. B.; Wijeratne, G. B.; Burr, A. D.; Parham, J. D.; Day, V. W.; Jackson, T. A., Steric and Electronic Influence on Proton-Coupled Electron-Transfer Reactivity of a Mononuclear Mn(III)-Hydroxo Complex. *Inorg Chem* **2016,** *55* (16), 8110-20.
2. Leto, D. F.; Chattopadhyay, S.; Day, V. W.; Jackson, T. A., Reaction landscape of a pentadentate N5-ligated Mn(II) complex with O2 - and H2O2 includes conversion of a peroxomanganese(III) adduct to a bis(mu-oxo)dimanganese(III,IV) species. *Dalton Trans* **2013,** *42* (36), 13014-25.
3. Lee, Y.; Jackson, T. A., Ligand Influence on Structural Properties and Reactivity of Bis(μ-oxo)dimanganese(III,IV) Species and Comparison of Reactivity with Terminal MnIV-oxo Complexes. *ChemistrySelect* **2018,** *3* (47), 13507-13516.
4. Sankaralingam, M.; Jeon, S. H.; Lee, Y.-M.; Seo, M. S.; Ohkubo, K.; Fukuzumi, S.; Nam, W., An amphoteric reactivity of a mixed-valent bis(μ-oxo)dimanganese(iii,iv) complex acting as an electrophile and a nucleophile. *Dalton Trans.* **2016,** *45* (1), 376-383.